Calcium-dependent regulation of auxin transport in plant development

Wei, X.

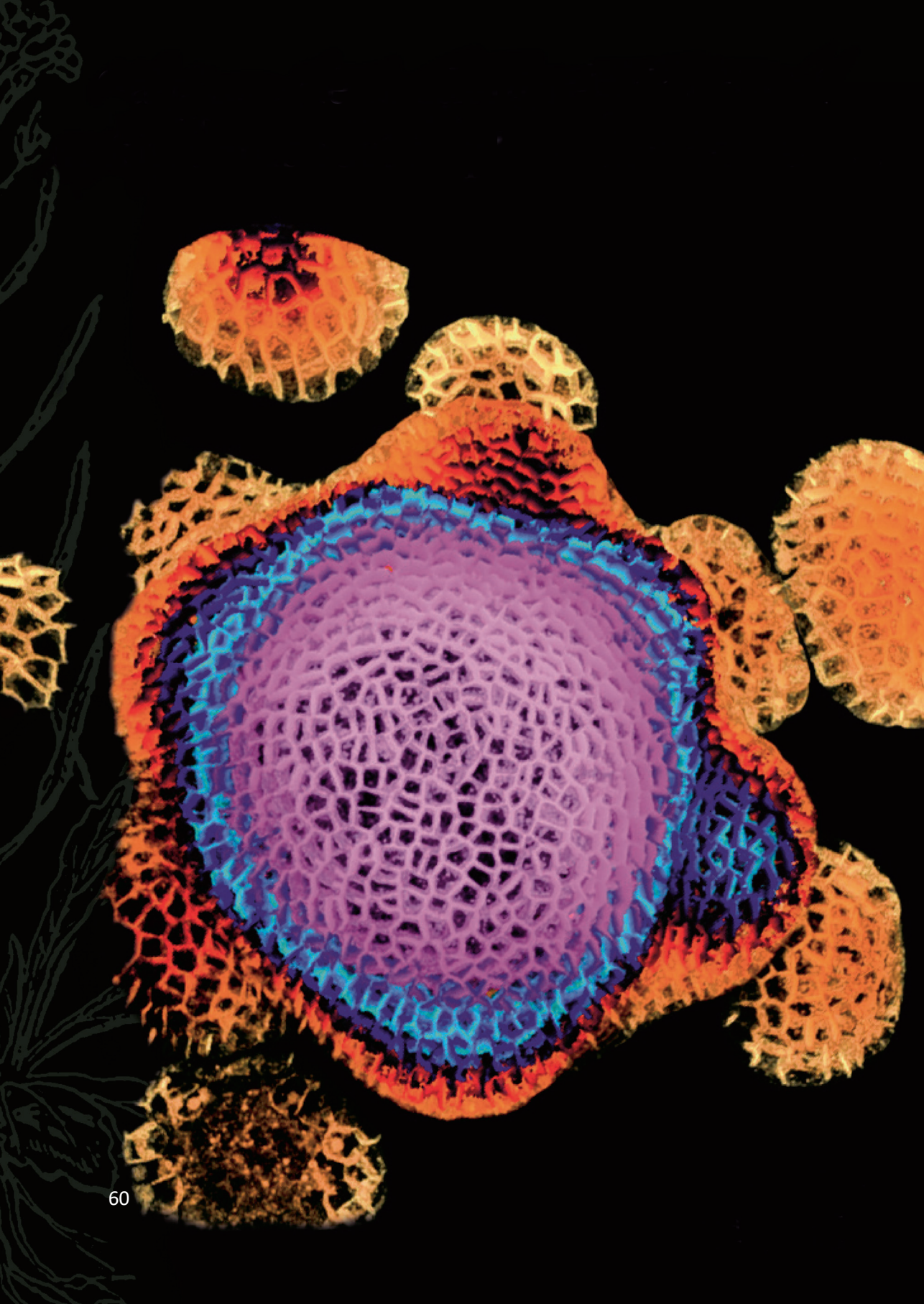

Chapter 2

CALMODULIN-LIKE 12/TOUCH 3 and closely related calmodulins and calmodulin-like proteins redundantly interact with the PINOID kinase

Xiaoyu Wei[1], Yuanwei Fan[1,2], Parjanya Kocherla[1], Linge Li[1,3] and Remko Offringa[1*]

[1] Plant Developmental Genetics, Institute of Biology Leiden, Leiden University, Sylviusweg 72, 2333 BE, Leiden, Netherlands

[2] Current address: Department of Biology and Center for Engineering Mechanobiology, Washington University in St. Louis, St. Louis, MO 63130, USA

[3] Current address: Plant Ecophysiology, Institute of Environmental Biology, Utrecht University, Padualaan 8, 3584 CH Utrecht, The Netherlands

[*]Author for correspondence: r.offringa@biology.leidenuniv.nl

The results in this Chapter are included in the following publication: Fan, Y.W., **Wei, X.Y**. ….Offringa, R*. Auxin-induced regulation of PIN polarity by calcium-dependent binding of calmodulins and calmodulin-likes to the PINOID kinase (submitted).

Abstract

Plants have evolved an intricate system to survive in their changing and often unfavourable environment due to their sessile nature. Cross talk between the plant hormone auxin, a key regulator of plant growth and development, and Ca^{2+}, a universal second messenger, has been proposed to transduce various environmental and endogenous signals and modulate developmental plasticity. The *Arabidopsis thaliana* (Arabidopsis) AGC3 kinase PINOID (PID) is a key regulator of polar auxin transport, acting as a binary switch in apical-basal polar targeting of PIN FORMED (PIN) auxin efflux carriers and thereby determining the direction of auxin flow. Previously, we identified the calmodulin-like (CML) protein CALMODULIN-LIKE 12/TOUCH 3 (CML12/TCH3) as interacting partner of PID, suggesting that PID is one of the hubs in the Ca^{2+}-dependent regulation of auxin action. Here we found that a confined clade comprising seven CaMs and four closely-related CMLs, including CML12/TCH3, interact with PID. In Arabidopsis protoplasts, co-transfection of these CaM/CMLs with PID in the presence of auxin resulted in PID disassociation from the plasma membrane. A comparative study on the spatio-temporal expression of the corresponding *CaM/CML* genes and *PID* using *promoter:GUS* reporter fusions displayed differential but also largely overlapping expression patterns in most tissues throughout all the developmental stages. Interestingly, *CaM2*, *CaM7*, *CML10* and *CML12/TCH3* respond to auxin treatment and gravistimulation. These results confirm our previous conclusion that calcium is an important second messenger in regulating the direction of auxin transport by external but also internal signals, such as auxin itself.

Keywords: Auxin, PINOID (PID) kinase, Calmodulins/calmodulin-likes (CaM/CMLs), CALMODULIN-LIKE 12/TOUCH 3 (CML12/TCH3), Protein-protein interaction, *Arabidopsis thaliana*

Introduction

Due to their sessile nature, plants are constantly exposed to a changing and often unfavourable environment (Anderson et al., 2011). To survive, they have evolved an intricate system to sense various environmental cues, and to transduce these cues into intracellular signalling thereby activating downstream physiological responses (Raza et al., 2020). One of the core signal transduction components in this environmental sensing system is the second messenger calcium (Ca^{2+}) (Dong et al., 2022).

Ca^{2+} is an essential macronutrient that plays an important role in plant growth and development, such as in the formation of cell walls, cell membranes and other cellular processes (Hepler and Wayne, 1985; Eklund and Eliasson, 1990; Xu and Heath, 1998). On the other hand, Ca^{2+} is universally involved in responses to environmental changes (Xu et al., 2022). Many environmental cues (light, abiotic and biotic stresses), and internal signals (e.g. plant hormones) elicit signal-specific and tissue-specific changes in the concentration of cytosolic Ca^{2+} ($[Ca^{2+}]_{cyt}$), which is defined as the 'calcium signature' (Dong et al., 2022; Xu et al., 2022).

The stimulus-specific information encoded in the calcium signature is relayed and deciphered through the action of sensor proteins that bind Ca^{2+} (Hashimoto and Kudla, 2011).The majority of Ca^{2+} sensors are small proteins that reversibly bind Ca^{2+} with high affinity, with one or more highly conserved helix-loop-helix motifs termed "EF hands" (Day et al., 2002; Sanders et al., 2002). Ca^{2+} sensors can be sorted into two major groups: the sensor relays and the sensor responders (Sanders et al., 2002; Hashimoto and Kudla, 2011). The sensor relays function through bimolecular interactions and comprise calmodulins (CaMs), calmodulin-like proteins (CMLs) and calcineurin-B like proteins (CBLs). They undergo a conformational change after binding with Ca^{2+}, which allows them to interact with target proteins, such as the Ca^{2+} and CaM-dependent protein kinase (CCaMK) and the CBL-interacting protein kinases (CIPKs), which subsequently respond by

changes in structure and (enzyme) activity (Hashimoto and Kudla, 2011). In contrast, the Ca^{2+}-dependent protein kinase (CDPK) are sensor responders that function through intramolecular interactions between the sensor (EF hand) and the kinase (responder) domain. Binding of Ca^{2+} results in activation of the kinase domain, leading to the subsequent phosphorylation of target proteins (Hashimoto and Kudla, 2011).

Among the Ca^{2+} sensors, the CaMs are the most extensively studied. CaMs are highly conserved, small, acidic, relatively stable proteins that are ubiquitously expressed in eukaryotic cells (McCormack et al., 2005). The *Arabidopsis thaliana* (Arabidopsis) genome harbours seven *CaM* genes encoding four CaM isoforms: CaM1/4, CaM2/3/5, CaM6, and CaM7 (McCormack et al., 2005). They share a similar protein structure of two globular domains, each of them containing a pair of EF-hands, connected by an α-helical linker domain (McCormack et al., 2005). In addition, the Arabidopsis genome encodes an extended family of CaM-like proteins (CMLs). These CMLs have between one to six EF hand motifs and no other identifiable functional domains (La Verde et al., 2018). And the difference in target specificity, subcellular localization and Ca^{2+} affinity of CMLs compared to CaMs indicate that they have evolved to diverse roles in Ca^{2+} signalling (La Verde et al., 2018).

Another important player in plant responses to environmental stimuli is the plant hormone auxin, or indole-3-acetic acid (IAA). Through the dynamic distribution of auxin minima and maxima within plant tissues, this hormone is involved in an impressive variety of plant biological processes, ranging from regulating basic processes such as cell expansion and cell division to orchestrating embryogenesis, tissue specification, and organ development (Gomes and Scortecci, 2021). The differential distribution of auxin is established and maintained through the combined action of biosynthesis, metabolism, and cell to cell polar auxin transport (PAT) (Mroue et al., 2018). PAT is mediated by three auxin transporter families, namely the PIN-FORMED (PIN) efflux transporters, the ATP-binding cassette B

(ABCB)-type efflux transporters, and AUXIN RESISTANT1/LIKE-AUX1 (AUX1/LAX) influx transporters (reviewed by Geisler, 2021). Among these transporters, the PIN auxin efflux carriers play a major role in determining the direction of auxin flow by their polar localization at the plasma membrane (PM) of the cell (Geisler, 2021). They are named after the *pin formed1* (*pin1*) loss-of-function mutant of one of the founding members, which shows severe defects in organ formation at the inflorescence meristem and as a result forms a needle-like inflorescences (Okada et al., 1991; Galweiler et al., 1998). The activity, polarity and trafficking of PINs are finely regulated by protein kinases that phosphorylate different residues in the central PIN hydrophilic loop (HL) (reviewed in Bassukas et al., 2022). Of these, the AGC3 kinases PINOID (PID), WAG1 and WAG2 instruct shootward/apical asymmetric PIN localisation by phosphorylating the serine residue in three conserved TPRXS motifs within the PIN-HL (Friml et al., 2004; Michniewicz et al., 2007; Huang et al., 2010; Dhonukshe et al., 2010). The *pid* loss-of-function mutant phenocopies the needle-like inflorescences of the *pin1* mutant, indicating that it is the dominant kinase regulating PIN1 polarity during organ formation in the inflorescence meristem (Bennett et al., 1995; Friml et al., 2004; Huang et al., 2010). More severe phenotypes, such as embryos without cotyledons and agravitropic roots, are only observed in the *pid wag1 wag2* triple mutant, showing that the three kinases act redundantly in these processes (Dhonukshe et al., 2010).

It has been reported that auxin acts in part through Ca^{2+} signalling, as cytoplasmic Ca^{2+} levels $[Ca^{2+}]_{cyt}$ rapidly increase after auxin application (Hasenstein and Evans, 1986; Gehring et al., 1990; Shishova and Lindberg, 2004; Monshausen et al., 2011). These changes in $[Ca^{2+}]_{cyt}$ were found to suppress PAT (Dela Fuente and Leopold, 1973) and to mediate gravitropic and phototropic growth responses (Baum et al., 1999; Plieth and Trewavas, 2002; Toyota et al., 2008a, b; Zhao et al., 2013) and organ formation at the shoot apical meristem (Li et al., 2019).

The finding that PID interacts with the CALMODULIN-LIKE 12/TOUCH 3 (CML12/TCH3) and the EF hand containing PID-BINDING PROTEIN 1 (PBP1) in a Ca^{2+} dependent manner provided a first molecular insight on how Ca^{2+} could possibly affect PAT (Benjamins et al., 2003). CML12/TCH3 is a negative regulator of PID kinase activity, both *in vitro*, as shown by phosphorylation assays, and in *planta* where *CML12/TCH3* overexpression reduces *PID* overexpression induced root meristem collapse (Robert, 2008; Galván-Ampudia, 2009). Moreover, when interacting with CML12/TCH3 in auxin-treated protoplasts, PID was sequestered from the PM to the cytosol (Galván-Ampudia, 2009). The same sequestration of PID was observed in root epidermis cells when roots were treated with auxin, and this sequestration was delayed, but not absent, in the *tch3* loss-of-function mutant. Moreover, the *tch3* loss-of-function mutant only shows a mild phenotype, strongly suggesting that CaMs and other CMLs function redundantly with CML12/TCH3. Here we observed that a confined clade comprising seven CaMs and the three CMLs (CML8, CML10, CML11) most closely related to CML12/TCH3 do also interact with PID. In Arabidopsis protoplasts, co-expression of these CaM/CMLs and PID in the presence of auxin resulted in dissociation of PID from PM. A systematic spatio-temporal expression study of the PID-interacting CaM/CMLs showed that their corresponding genes display a largely overlapping expression pattern with *PID* and that, like *PID, CaM2*, *CaM7*, *CML10* and *CML12*/*TCH3* are auxin responsive.

Results

PID interacts with CML12/TCH3 and 10 closely related CaMs and CMLs

CML12/TCH3 was previously identified as a PID interacting protein in a yeast-two hybrid screen, and the Ca^{2+}-dependent interaction was confirmed by *in vitro* pull-down assays (Benjamins et al., 2003; Galván-Ampudia, 2009). As the analysis of the *tch3* loss-of-function mutant suggested that other CMLs and possibly CaMs

might act redundantly with CML12/TCH3 (Robert, 2008; Fan, 2014), we selected the most closely related homologs of CML12/TCH3, including seven CaMs, CML8, 9, 10, 11, 13 and CML14 and the more distantly related CML24/TCH2 as candidates. *In vitro* pull-down assays using GST-tagged PID bound to glutathione beads as bait and His-tagged CaM/CMLs as prey indicated that the seven CaMs and CML8, 10 and CML11 interacted with PID, but that CML9, 13 and 14 and the more distantly related CML24 did not (Figure 1A; Figure S1).

Bimolecular fluorescence complementation (BiFC) was used to confirm these results for CaM1, CML10 and CML12/TCH3, using CML9 and CML24 as negative controls. Co-expression of PID-VYCE (having the C-terminus of Venus fused to PID) and CaM/CMLs-VYNE (N-terminus of Venus fluorescent protein fused to CaM1, CML9, CML10, CML12/TCH3 or CML24) in *Nicotiana benthamiana* leaf epidermis cells showed that CaM1, CML10 and CML12/TCH3 interact with PID, whereas CML9 and CML24 do not (Figure 1B). Subsequent co-transfection of *p35S:PID-GFP* and *p35S:CaM/CMLs-mRFP* in Arabidopsis protoplasts supplemented with auxin showed strong PID sequestration from the PM in protoplasts co-expressing one of the seven CaMs or the closely related CML8, 10 and CML11, whereas co-expression of the more distantly related CML9, 13, 14 and CML24 did not lead to sequestration of PID from the PM (Figure 1C).

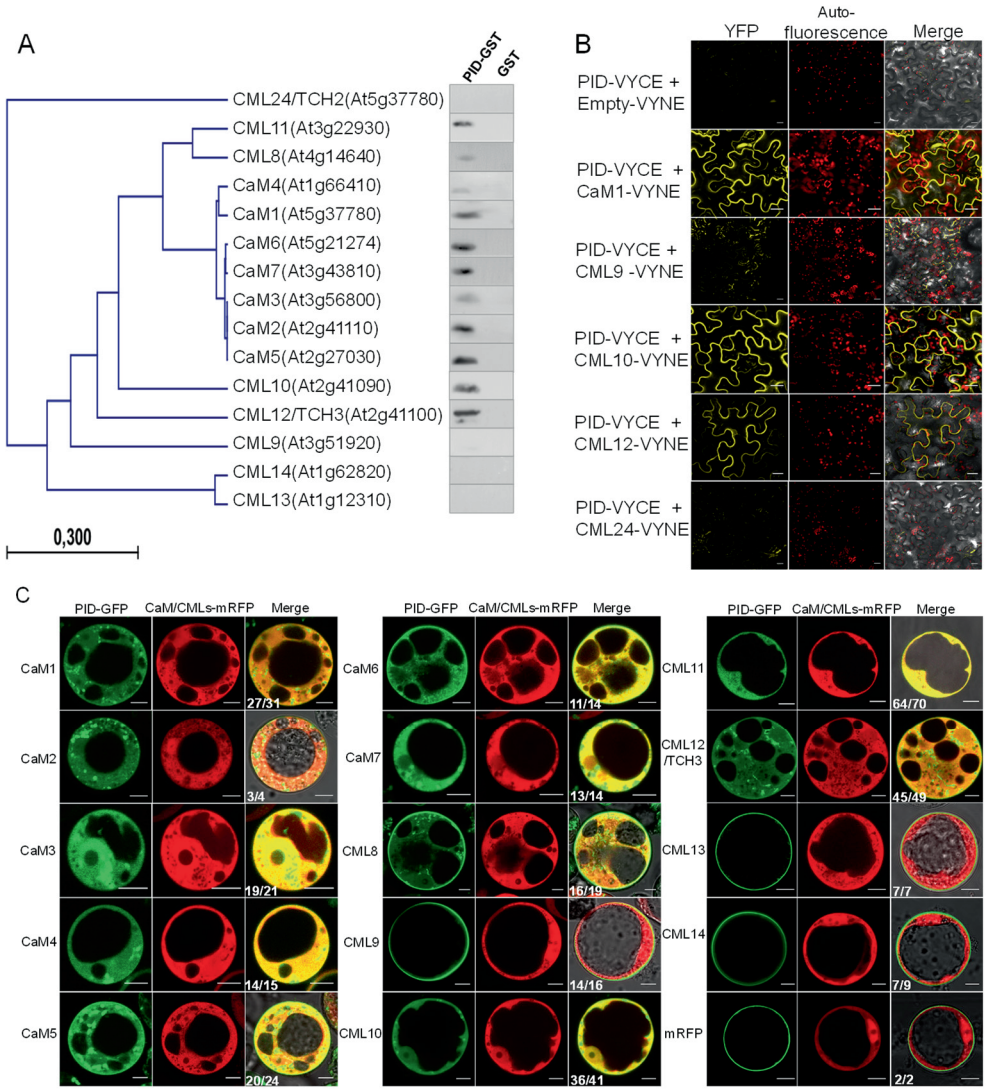

Figure 1. PID interacts with CML12/TCH3 and 10 closely related CaMs and CMLs. (**A**) Phylogenetic tree combined with the results of *in vitro* pull-down experiments using GST or GST-tagged PID bound to glutathione beads as bait and His-tagged CaMs or CMLs as prey. The phylogenetic tree was constructed based on the full-length protein sequences using the UPGMA method in CLC Main Workbench 6. Pulled down CaMs/CMLs are detected by hybridizing the Western blot with anti-His antibodies. (**B**) Bimolecular Fluorescence Complementation (BiFC) assay performed by co-expression of the indicated combination of fusion proteins (PID-VYCE: PID C-terminally fused to the C-terminal half of Venus; CaM/CML-VYNE: CaM/CML C-terminally fused to the N-terminal half of Venus) in leaf epidermis cells of three weeks old *Nicotiana benthamiana* plants after *Agrobacterium*-mediated DNA transfer. (**C**) *35S* promoter-driven co-expression of PID-GFP and CaM/CML-mRFP fusions in Arabidopsis protoplasts in the presence of auxin. Sequestration

of PID to the cytosolic is indicative of an interaction (CaM1-7, CML8, 10,11,12), whereas PM-localization of PID indicates that there is no interaction (CML9, 13 and 14 and the mRFP control). White numbers indicate how many of the total number of images show the same result. Scale bars indicate 10 µm in **(B)** and **(C).**

The above results validated our hypothesis and showed that a confined clade comprising the seven CaMs and four CMLs-CML8, 10, 11 and CML12/TCH3 act redundantly in interacting with and regulating the PID kinase, and that the more distantly related CMLs do not. The data explain why the *tch3* and other *cam/cml* single loss-of-function mutants do not present any eye-detectable phenotype (Figure S2).

Analysis of the structural diversity of both the interacting and non-interacting CaMs and CMLs using the online tool Multiple Em for Motif Elicitation (MEME) suite (http://meme-suite.org/tools/meme) showed that, except for CML12/TCH3, most proteins contain four Ca^{2+}-binding EF-hands, each characterized by a conserved signature motif (1 to 4), and lack additional functional domains (Figure 2). CML12/TCH3 is exceptional as it contains six EF-hands due to a duplication of the first two EF-hands (Figure 2B). We did not detect a difference in EF-hand motif order or composition or a clear difference in the amino acid sequence that distinguishes the PID interacting from the non-interacting CaMs/CMLs.

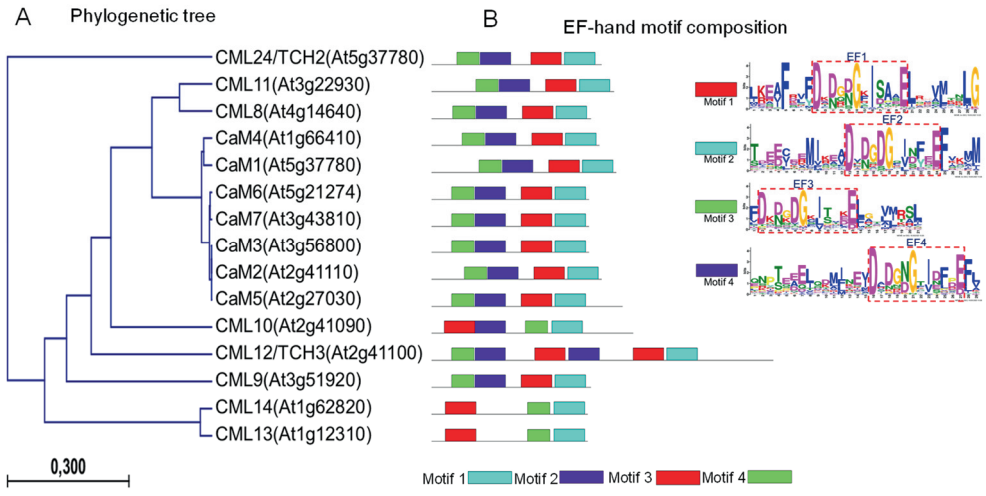

Figure 2. Phylogenetic tree and protein structure of the PID-interacting and not interacting CaM/CMLs in Arabidopsis. (**A**) A phylogenetic tree of PID-interacting and representative non-interacting CaMs and CMLs constructed based on the full-length protein sequences using the UPGMA method in CLC Main Workbench 6. (**B**) EF-hand motif composition of the CaM and CML proteins in (**A**). Four conserved motif signatures were identified in the EF-hands of Arabidopsis CaMs and CMLs using the Multiple Em for Motif Elicitation (MEME) suite (http://meme-suite.org/tools/ meme) (Bailey and Elkan, 1994) with standard searching parameters, allowing a maximum of four different motifs and an optimum motif width between six and 30 amino acids.

PID interacting CaM/CMLs display a largely overlapping expression pattern

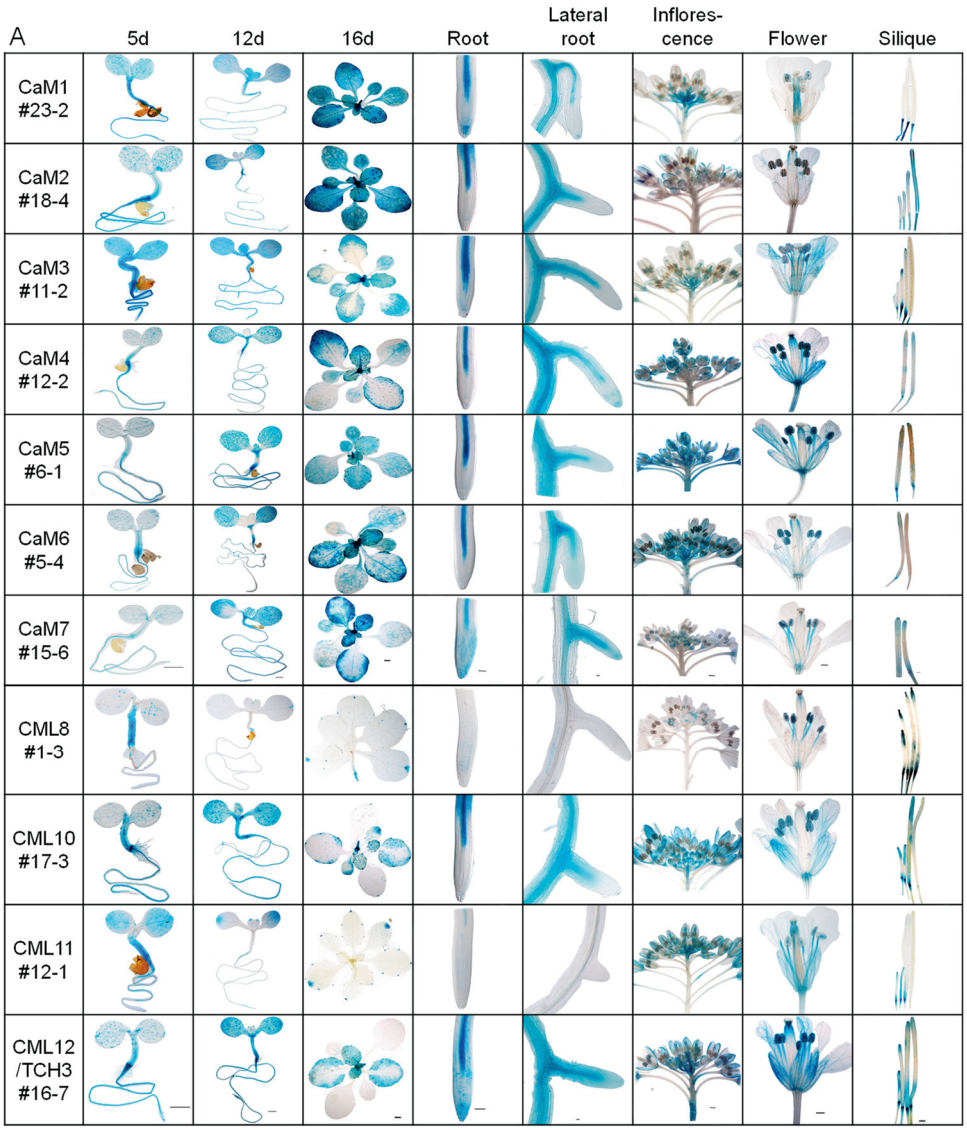

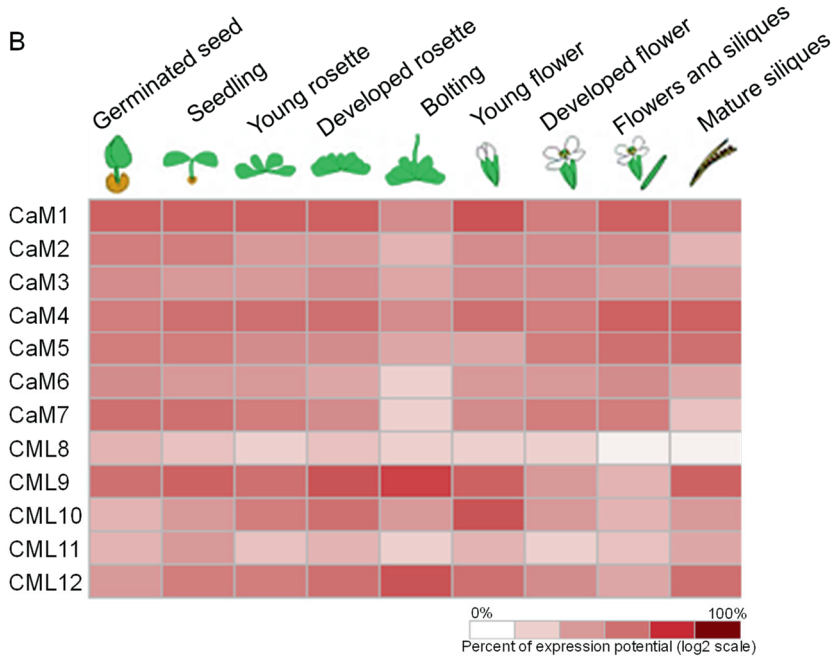

Figure 3. Spatio-temporal expression pattern of *CaM* and *CML* genes encoding PID-interacting proteins. (**A**) Histochemical staining for GUS activity in 5-, 12-, and 16-day-old *pCaM/CML:turboGFP-GUS* seedlings/plants and different tissues. # and number indicate the transgenic line number. Scale bars in 5-, 12-, and 16-day-old seedlings/plants, root, lateral root, inflorescence, flower, silique indicate 1 mm, 5 mm, 5 mm, 200 µm, 50 µm, 5 mm, 1 mm, 5 mm, respectively. (**B**) Relative expression heat map for the indicated Arabidopsis *CaMs* and *CMLs* in different tissues and developmental stages obtained from Genevestigator. Developmental stage from left to right: germinated seed, seedling, young rosette, developed rosette, bolting, young flower, developed flower, flowers and siliques, and mature siliques.

Previous analysis of the *CML12/TCH3* expression pattern has shown that the gene is expressed in the shoot apical meristem, vascular tissue and the pericycle at positions of lateral roots emergence, and in root and leaf cells undergoing cellular expansion (Sistrunk et al., 1994, Antosiewicz et al., 1995, Robert, 2008). In addition, *TCH3* expression was shown to be strongly induced by auxin and touch, especially in the root tip (Braam and Davis, 1990; Antosiewicz et al., 1995; Benjamins et al., 2001; Fan, 2014). It has also been reported that *PID* is co-expressed with *TCH3* in epidermis cells of the elongation zone of the root tip, vascular tissue and in the shoot apical meristem (Benjamins et al., 2001; Benjamins

et al., 2003), allowing a possible functional interaction between the two proteins in these tissues. In fact, auxin treatment has been shown to lead to Ca^{2+}-dependent sequestration of a functional PID:VENUS fusion from the PM to the cytosol in root epidermis cells. The sequestration was delayed in *tch3* loss-of-function mutant roots (Fan, 2014), suggesting that CML12/TCH3 does have a role in this.

To investigate which other PID interacting CaM/CMLs are also expressed in the PID expression domain, we studied the spatio-temporal expression patterns of these *CaM/CML* genes using lines transgenic for *pCaM/CMLs:turboGFP-GUS* fusions. Histochemical staining of different tissues at different developmental stages for GUS activity showed that the seven *CaM* genes share striking similarities in expression pattern. Although there is some variation in specific tissues, all genes are expressed in roots, hypocotyls, cotyledons and leaves, with predominant expression in vascular tissue, inflorescence meristems, flowers and siliques. Also in the root tip there is mild diversity in expression pattern, as *CaM1*, *3, 4, 5*, and *7* show clear expression in the quiescent center (QC) of the root apical meristem (RAM) and in the columella cells to a varying extent. Additionally, *CaM7* is also expressed in the epidermis of the root tip (Figure 4A). In contrast, the *CMLs* show much more diversity compared to the *CaMs*. At the seedling stage, *CML8*, *10*, *11*, and *CML12/TCH3* are expressed in the cotyledons, hypocotyl, and the root vasculature, of which, *CML8* shows a relatively weak expression in cotyledons but stronger in the hypocotyl. However, in adult leaves, *CML8* and *CML11* specifically express in the tip of the leaves, while *CML10* and *CML12/TCH3* express in the young developing leaves. In roots, *CML8* and *CML11* are weakly expressed in the epidermis of the elongation zone, whereas *CML12/TCH3* expression here is much stronger and broader. Like the *CaM* genes, all four *CML* genes are expressed in flowers and siliques, but much weaker for *CML8*. Together with data compiled from the GENEVESTIGATOR database (Figure 3B), these results show that the genes encoding PID interacting

CaM/CMLs display a largely overlapping expression pattern and are generally expressed in almost all tissues throughout all developmental stages.

Four genes encoding PID-interacting CaM/CMLs are auxin responsive and induced during gravitropic growth

Previous studies have indicated that both *PID* and *CML12/TCH3* are auxin responsive (Antosiewicz et al., 1995; Benjamins et al., 2001; Benjamins et al., 2003; Fan, 2014). In the case of *CML12/TCH3*, its auxin responsive expression in epidermis cells of the root tip would increase CML12/TCH3 levels and thereby potentiate its (auxin-induced) repressive effect on PID activity by binding to and sequestering PID from the plasma membrane (Fan, 2014). To test if the other genes encoding PID interacting *CaM/CMLs* are also auxin responsive, we treated 5-day-old seedlings of the corresponding *pCaM/CML:turboGFP-GUS* reporter lines for 1, 2, 3 and 5 hours with auxin and histochemically stained for GUS activity.

Four of the twelve *CaM/CML* genes showed a clear auxin responsive gene expression. In line with previous findings, *CML12/TCH3* expression was strongly induced in the entire root tip after one hour of auxin treatment, and the expression became more intense in the root tip, hypocotyl, shoot apex and cotyledons at later time points (Antosiewicz et al., 1995; Benjamins et al., 2001; Benjamins et al., 2003; Fan, 2014). *CaM2*, *CaM7* and *CML10* generally shared this pattern of auxin responsive gene expression, but the induction in root tips was less intense for *CaM7* and limited to the elongation zone of the root tip for *CaM2* and *CML10*.

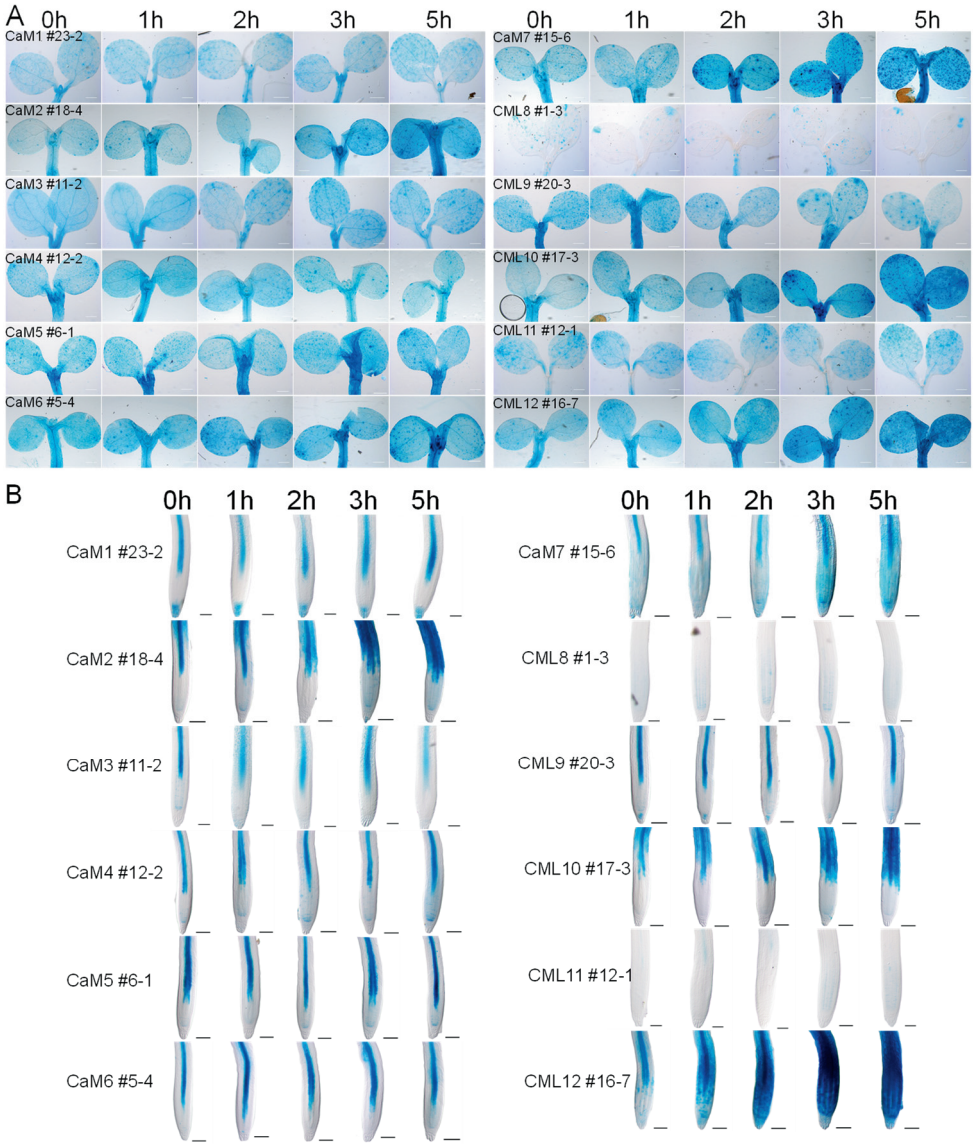

Figure 4. Four of the genes encoding PID-interacting CaM/CMLs are auxin responsive in seedling shoots and root tips. (A-B). Histochemical staining of the shoot **(A)** and root tip **(B)** of 5-day-old *pCaM/CMLs:turboGFP-GUS* seedlings treated with 5 µM IAA for 0, 1, 2, 3, or 5 hours. Images representative of three to five replicates are shown. Scale bars in **(A)** and **(B)** indicate 50 mm, 50 µm, respectively. # and number indicate the transgenic line number.

Interestingly, the expression of the auxin responsive genes was also enhanced during root gravitropic growth (Figure 5). For *CAM2* and *CML10*, this enhancement was restricted to the root elongation zone with predominant induction in the vascular tissue, consistent with their limited auxin responsive expression in the root tip (Figure 4B). As previously shown for *CML12/TCH3* (Fan, 2014), during the gravitropic response *CAM7* expression was enhanced in the entire root tip with highest expression in the epidermal cells at the lower side of the root, in line with the transient asymmetric auxin distribution during the root gravitropic response (Band et al., 2012).

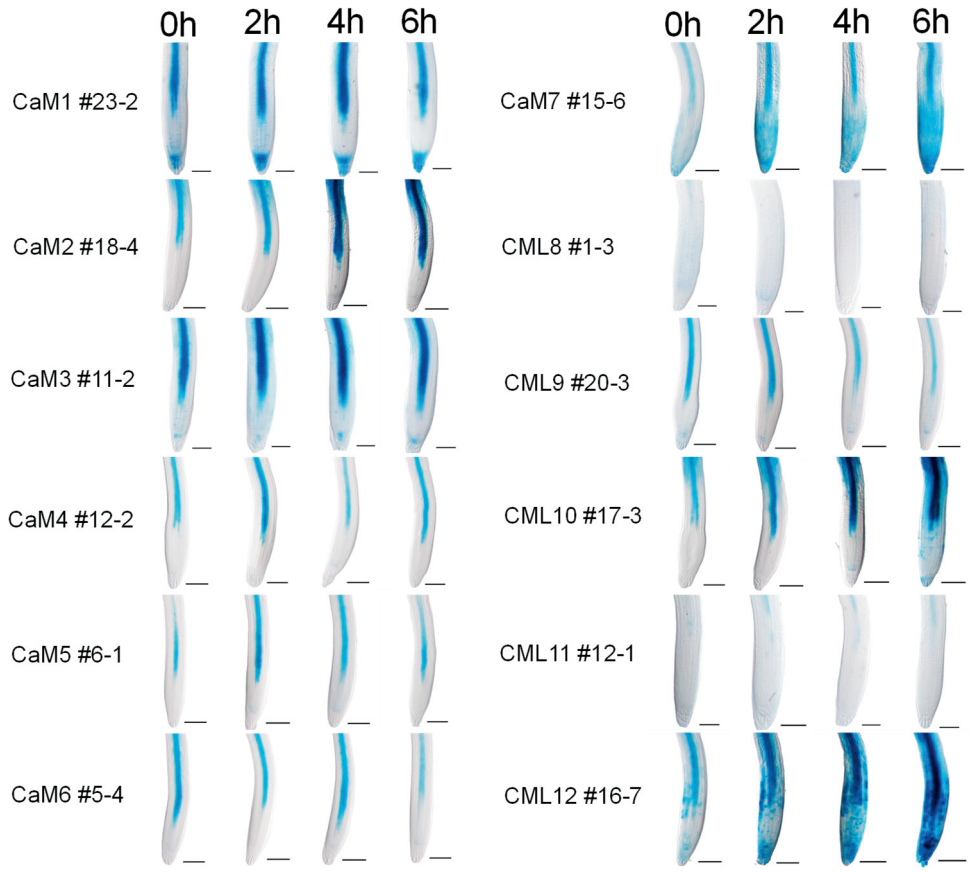

Figure 5. The expression of the auxin responsive CaM/CML genes is induced in the root tip during gravitropic growth. *pCaM/CMLs:turboGFP-GUS* seedlings were grown on vertical plates

containing agar medium for five days, transferred to new vertical agar medium plates, and gravi-stimulated by tilting the plates 90 degrees. Seedlings were histochemically stained for GUS activity after 0, 2, 4 or 6 hours incubation. # and number indicate the transgenic line number.

These results suggest that specifically CAM7 acts redundantly with CML12/TCH3 with respect to the previously observed PID sequestration in epidermis cells in the root tip. The stronger expression of CML12/TCH3 suggests that this is the more important CAM/CML in this process, which might explain the observed delay in auxin-induced PID sequestration in the *tch3* loss-of-function mutant background (Fan, 2014).

Discussion

The perception of environmental signals and internal cues such as gravity and auxin by plant cells generally leads to oscillations in the $[Ca^{2+}]_{cyt}$ (Felle, 1988; Gehring et al., 1990; Plieth and Trewavas, 2002; Toyota et al., 2007, 2008a, b; Verma et al., 2022). These stimulus-specific transient Ca^{2+} signatures are deciphered by Ca^{2+} sensors, such as CaMs and CMLs. Previously, we identified a possible mechanism by which auxin regulates its own polar transport. We observed that the AGC kinase PID, which regulates PAT by phosphorylating the PIN auxin efflux carriers, is inactivated and sequestered from the PM through an auxin-triggered, Ca^{2+}-dependent interaction with CML12/TCH3 (Benjamins et al., 2003; Galvan-Ampudia, 2009; Fan, 2014). As the *tch3* loss-of-function phenotype did not show clear phenotypes (Fan, 2014), we suspected that other CMLs and/or CaMs would act redundantly with CML12/TCH3. Here we found that seven CaMs and three other CMLs, all belonging to a confined clade that includes CML12/TCH3, also interact with PID and are able to sequester the kinase from the PM. The largely overlapping spatio-temporal, and for some auxin responsive, expression of the corresponding genes supports the notion that they may act redundantly in regulating the PID kinase.

Redundant action of CaM/CMLs in regulating target proteins seems a general concept

A protein microarray screen, genetic analysis and *in vivo* studies have shown that CaM/CMLs binding proteins generally interact with more than one CaM/CMLs (Popescu et al., 2007; Oh et al., 2012; Sun et al., 2022). In fact, the protein microarray screen has shown that about 25% (44 of 173) of the CaM/CML target proteins interact with all six CaM/CMLs that were used in this screen (CaM1, CaM6, CaM7, CML8, CML9, CML10), whereas 50% of the proteins bound to two or more of these CaM/CMLs (Popescu et al., 2007).

In the case of PID, there seems to be some specificity, as it interacts with a confined clade comprising CAMs and the four most closely related CMLs, and no interaction was observed between PID and the more distantly related CML9, 13, 14 and CML24 (TCH2). As a result, the non-interacting CMLs did not sequester PID from the PM to cytosol. The fact that the capacity to regulate PID kinase activity is limited to a specific subclade of the CaM/CMLs family suggests some structural conservation among the PID-interacting CaM/CMLs. Unfortunately, protein alignment and a careful search for differences in the conserved EF-hand motif type or order did not detect clear differences between the interacting and not-interacting CaM/CMLs. This indicates that functional studies on this interaction from the CaM/CML side will be difficult, if not impossible, also in view of the promiscuous interactions of CaM/CMLs with other target proteins (Popescu et al., 2007; Oh et al., 2012; Sun et al., 2022). Nonetheless, based on our expression analysis, only CAM7 and CML12/TCH3 show clear expression in epidermis cells of the differentiation zone of the root tip following auxin treatment or gravistimulation, suggesting that a *cam7 cml12/tch3* double mutant might reveal a mutant root phenotype. Unfortunately, time limitation did not allow to test this hypothesis. Based on the analysis presented in this Chapter, we decided to study the functional relevance of the PID CaM/CML interaction from the PID side. These follow-up studies are described in Chapter 3 and 4 of this thesis.

Limited functional diversification between genes encoding PID interacting CaM/CMLs

Our study on the spatio-temporal expression of the genes encoding PID-interacting CaM/CMLs showed that the seven *CaMs* are universally expressed in most organs (Figure 3A). On the one hand, this finding fits their role as the major Ca^{2+} sensors that regulate the activity of plentiful downstream target proteins involved in wide range of developmental processes and responses (La Verde et al., 2018). On the other hand, it is difficult to explain how these CaMs have maintained their high protein sequence identity combined with their largely overlapping spatio-temporal expression pattern under strict natural selection. One possibility is that, because of their promiscuous role, there is a requirement for a high CaM protein level in the cell beyond the capacity of one or a few *CaM* genes. The other possibility is that the seven *CaM* genes are the result of more recent gene duplication events and that there has not been sufficient time for their sub-functionalisation.

Compared to the *CaM* genes, the three genes encoding PID-interacting CMLs do show more diversification. *CML8* and *CML11* are highly expressed in the hypocotyl at early developmental stages, and later the expression becomes limited to the root-shoot junction, leaf tip and flowers. Our observations on the *CML8* expression pattern is similar to what was reported by Zhu et al. (2017). Here, the authors showed that *CML8* plays a role in plant immunity against *Pseudomonas syringae* in a salicylic acid dependent manner. *CML10* is strongly expressed in the root, hypocotyl and cotyledons of young seedlings and flowers. In rosette leaves, *CML10* is mainly accumulating in the newly formed leaves, indicating a possible role in early leaf development. *CML10* has been reported to be crucial in coping with biotic and abiotic stresses, and its expression is induced by bacterial (*Pseudomonas syringae*), fungal (*Plectosphaerella cucumerina*) and oomycetal (*Hyaloperonospora parasitica*) pathogens (Zimmermann et al., 2004; McCormack et al., 2005), H_2O_2 (McCormack et al., 2005; Cho et al., 2016), cold stress (Yu et al., 2022) and auxin (Figure 4). The expression pattern of *CML12/TCH3* is consistent

with previous research, mainly in the vascular tissues of roots, cotyledons, hypocotyl, flowers and in the young developing rosette leaves. Additionally, *CML12/TCH3* is also expressed in the epidermis of the elongation zone of the root tip. As a touch-responsive gene, the expression of *CML12/TCH3* can be induced by touch, wind, rain, wounding, darkness (Braam and Davis, 1990; Sistrunk et al., 1994; Wright et al., 2002), gravity (Figure S3) and auxin (Antosiewicz et al., 1995; Benjamins et al., 2001; Benjamins et al., 2003; Fan, 2014; Figure 4). These results indicate that CML12/TCH3 plays a crucial role in transducing both external and internal signals causing elevation of the $[Ca^{2+}]_{cyt}$. Recently, CML12/TCH3, CAM1, CAM4 and CAM6 have also been reported to cooperate with calcium-dependent protein kinases to trigger calcium-dependent activation of CaM-BINDING PROTEIN 60-LIKE G in the regulation of fungal resistance in Arabidopsis (Sun et al., 2022).

In conclusion, although the PID interacting CaMs and CMLs are seemingly redundant and involved in a plethora of responses, more detailed research is likely to reveal that they have sub-functionalized with both specific and overlapping roles in plant development and defence.

PID-CaM/CML-mediated Ca^{2+} signalling: another feedback loop by which auxin regulates its own action

Accumulating evidence has shown that PAT is regulated by various internal and external cues that trigger Ca^{2+} signalling, which in turn modulates PIN subcellular re-localization and trafficking. An inositol trisphosphate-induced increase in $[Ca^{2+}]_{cyt}$ was shown to modulate auxin transport by inducing apolarity of PIN1 but not of PIN2 (Zhang et al., 2011). Mechanical stimulation of SAM cells using glass needle-induced cell ablation triggers the increase of $[Ca^{2+}]_{cyt}$ and regulates the polarity of PIN protein, indicating the importance of Ca^{2+} in shoot development (Li et al., 2019). An auxin-induced increase in $[Ca^{2+}]_{cyt}$ has been reported in many species (Hasenstein and Evans, 1986; Felle, 1988; Shishova and Lindberg, 2004;

Monshausen et al., 2011), indicating the importance of Ca^{2+} in auxin physiology. It was shown to be required for the inhibition of auxin on root growth (Shih et al., 2015) and auxin-regulated root hair growth (Dindas et al., 2018). However, the downstream targets of auxin-induced Ca^{2+} signalling are still largely unknown.

The gravistimulation-induced increase in $[Ca^{2+}]_{cyt}$ in cells at the lower side of the root tip (Plieth and Trewavas, 2002; Toyota et al., 2007, 2008a, b) coincide with the asymmetric movement of auxin to this side (Lee et al., 1984; Band et al., 2012). At the same time the enhanced auxin levels result in the induction of *CML12/TCH3* expression (Antosiewicz et al., 1995; Monshausen et al., 2011; Chapters 3 and 4). Our results now suggest that CML12/TCH3 together with CAM7 are the receptors in the lower epidermis of the root tip that are activated by the elevated cytosolic Ca^{2+}, and as a result sequester PID and WAG2 from the PM to the cytosol (Figure 1C; Fan, 2014). Dissociation of these AGC kinases from the PM and their inactivation causes an apolarization of PIN2 at the lower side of root tip, thereby enhancing the asymmetric auxin distribution and thus the root gravitropic response (Fan, 2014). These results reveal yet another mechanism by which auxin regulates its own action.

Material and Methods

Molecular cloning and constructs

The constructs *pET16H-TCH3, pGEX-PID, pDONR207 PID* were described previously (Benjamins et al., 2003). *p35S:PID-GFP* was described in (Yao, 2019). To obtain the plasmids encoding His-tagged CaM/CMLs, the corresponding coding regions were amplified from cDNA of 5-day-old seedlings using the primer sets *CaM/CML attB F* and *CaM/CML attB R* (Table S1). The resulting DNA fragments were subsequently recombined into *pDONR207* (Invitrogen, Gateway cloning, BP reaction) and *pET16H* (LR reaction). To generate the constructs *p35S:CaM/CML-mRFP* and *pDEST-CaM/CML VYNE*, coding regions without stop codon were amplified from cDNA of 5-day-old seedlings using the primer set CaM/CML- attB F and CaM/CML-stop attB R (Table S1), the resulting fragments were first recombined into *pDONR207* (BP reaction) and subsequently into *p35S:mRFP* or *pDEST-^{GW}VYNE* (LR reaction). *pDEST-PID VYCE* resulted from the LR reaction of *pDONR207 PID* and *pDEST-^{GW}VYCE*. To generate the constructs *pCaM/CML:turboGFP-GUS*, the corresponding promoter regions of selected CaM/CMLs were cloned using the primer sets pCaM/CMLs attB F and pCaM/CML attB R (Table S1), and then recombined into *pDONR207* (BP reaction) and from there into *pMDC163(gateway):turboGFP-GUS* (reconstructed by Yao 2019) (LR reaction).

Primers used were designed with CLC Main Workbench (CLC bio) software and listed in the Table S1.

Plant material and growth conditions and phenotype analysis

All transgenic lines and mutants used in this study are in the Columbia (Col-0) background. T-DNA insertion lines *cam1-1 (SALK_202076C), cam1-2 (GK-533G05), cam2-1 (SALK_114166C), cam2-2 (SALK_089283C), cam3-1 (SALK_149754C), cam4-1 (SALK_021224), cam4-2 (SAIL_736_D07), cam5-1*

(SAIL_595_D04), cam5-2 (SALK_007371C), cam6-1 (SALK_033803C), cam7-1 (SAIK_074336C), cml8-1 (SALK_02252C), cml8-2 (SALK_114570), cml10-1 (SALK_058561C), cml11-1 (SALK_083435C), cml12-1 (SALK_098779) were ordered from the Nottingham Arabidopsis Stock Centre.

To generate the *pCaM/CML:turboGFP-GUS* reporter lines, binary vectors were introduced into *Agrobacterium tumefaciens* strain AGL1 by electroporation (den Dulk-Ras and Hooykaas, 1995) and transformed in *Arabidopsis thaliana* Col-0 using the floral dip method (Clough and Bent, 1998).

For the seeds grown on plates, seeds were sterilized by 1min 70% ethanol, 10 min bleach solution containing 1% chlorine and washed three times with sterile H_2O. Sterilized seeds were kept in H_2O in the dark at 4 °C for two days for vernalization and germinated on vertical plates with 0.5x Murashige and Skoog (1/2 MS, Duchefa) medium containing 0.05% MES, 1% sucrose, solidified with 1% Daishin agar (Duchefa) at 22 °C and 16 hours photoperiod. *Arabidopsis thaliana* plants grown on soil were cultured at 21 °C, 16 hours photoperiod and 70% relative humidity. *Nicotiana benthamiana* seeds were germinated on soil and plants were grown at 25 °C, and 70% relative humidity and 16 hours photoperiod.

Histochemical staining and microscopy

For histochemical staining, 5- and 12-day-old *pCaM/CML:turboGFP-GUS* seedlings or tissues from plants at different developmental stages were collected and fixed in 90% acetone at -20 °C for 20 min, followed by two times 10 min in GUS-washing solution (0.1 M PhospH-Pi buffer (0.1 M NaH_2PO_4 and 0.1 M Na_2HPO_4) pH 7.0, 10 mM EDTA, 2 mM $K_3Fe(CN)_6$) under vacuum and 10 minutes in GUS staining buffer (10 mM EDTA, 50 mM sodium phosphate pH 7.0, 1 mg/ml X-gluc, 0.1% (v/v) Triton X-100, 0.5 mM $K_3Fe(CN)_6$, 0.5 mM $K_4Fe(CN)_6$) under vacuum. Samples were subsequently stained for 3 hours at 37 °C in the dark. Staining was stopped by replacing the staining buffer for acetic acid/EtOH (3:1) for 60 minutes and by subsequent rehydration in a graded of ethanol series (75, 50,

25%) for 30 min each time. For the final step, 25% ethanol was replaced by water. For microscopy, stained seedlings and tissues were prepared on slides with chloralhydrate solution (4 : 2 : 1 (w/w) chloral hydrate : glycerol : water) and pictures were taken using a Leica MZ16FA microscope equipped with a Leica DFC 420 C digital colour Camera. Images were processed using Image J and assembled into figures using Adobe Photoshop.

Auxin treatment

Seeds were germinated on vertical plates containing solid 1/2 MS medium for five days, then transferred to liquid 1/2 MS medium supplemented with 5 μM IAA for 0, 1, 2, 3 or 5 hours. Because IAA was dissolved in DMSO at a 5 mM concentration, liquid medium containing 0.1% DMSO was used as control. Histochemical staining was performed, and pictures were taken as described above. Treatments were repeated three times.

Gravistimulation

Seeds were germinated on vertical plates containing solid 1/2 MS medium for five days, then transferred to fresh medium with the roots as straight as possible and allowed to recover for two hours. Gravistimulation was started by rotating the plates 90^{o}. Seedlings were harvested at 0-, 2-, 4-, and 6-hours after the start of gravistimulation and histochemical staining was performed and pictures were taken as described above. Experiments were repeated three times.

Protoplast transformation

Protoplasts were obtained from *Arabidopsis thaliana* Col-0 cell suspension cultures and transfected as described (Schirawski et al., 2000). Plasmid DNAs were extracted using the Plasmid Midi Kit (QIAGEN, #12143). For PEG-mediated transfection 10μg of each plasmid (*p35S:CaM/CML-mRFP* and/or *p35S:PID-turboGFP*) was added per 0.5×10^{6} protoplasts. The transfected protoplasts were

incubated for 16 hours at 21 °C in the dark. Pictures were taken using the Zeiss LSM5 Exciter/Axio Observer confocal microscope with either a 40x or 63x oil immersion objective (NA=1.2). The GFP signal was detected using an argon 488 nm laser for excitation and a 505 to 530 nm band pass emission filter. The RFP signal was detected using an argon 543 nm laser for excitation and a 560 to 615 nm band pass emission filter.

***In vitro* pull-down assay**

In vitro pull-down assays were performed as described (Robert, 2008) with some minor modifications. *E. coli* strain Rosetta (Novagen) was transformed with *pET16H-CaM/CML* or *pGEX-PID*. Single colonies were picked and grown overnight (o/n) at 37 ºC in 2 ml liquid LC medium complemented with 15 µg/ml Kanamycin (Km) or 35 µg/ml Chloramphenicol (Cam), respectively. The 2 ml cultures were sub-cultured in 100 ml fresh LC medium containing Cam and Km and grown at 37ºC until an OD_{600} of 0.6. Protein expression was induced with 1 mM IPTG for 4h at 30ºC. Bacteria were harvested by centrifugation at 4000 RPM for 20 minutes and frozen in liquid nitrogen. Frozen bacterial pellets were resuspended in 4 ml GST-tagged protein Extraction Buffer (20 mM Tris pH 7.5, 500 mM NaCl, 5 mM EDTA, 1 mM EGTA, 1 mM DTT, 0.2 % Triton X-100, 0.05 % Tween-20) or His-tagged protein Extraction/Binding Buffer (20 mM Tris pH 7.5, 500 mM NaCl, 5 mM $MgCl_2$, 2 mM $CaCl_2$, 1 mM DTT, 0.2 % Triton X-100, 0.05 % Tween-20) supplemented with 0.1 mM Phenylmethanesulfonylfluoride (PMSF) and a protease inhibitor tablet. The suspensions were sonicated for 2 minutes and centrifuged at 10000 g for 10 min at 4 ºC. For pull-down, 200 µl GST-PID supernatants was added to 200 µl of pre-equilibrated Pierce™ Glutathione Agarose beads (#16100, Thermo Scientific™) and samples were incubated for 2 h at 4ºC. Beads were washed twice with 1 ml Washing Buffer 1 (10 mM Tris pH 7.5, 150 mM NaCl, 5 mM EDTA, 1 mM EGTA, 1 mM DTT) after which 400 µl His-CaM/CML supernatants and 100 µl Extraction/Binding Buffer were added. The

mixture was incubated at 4°C for 4 hours on a rotator, the beads were washed twice with 500 µl Washing Buffer 2 (10 mM Tris pH 7.5, 150 mM NaCl, 5 mM $MgCl_2$, 2 mM $CaCl_2$, 1 mM DTT) and associated proteins were released by adding 30 µl 2× SDS loading buffer (2 mL Tris (1 M, pH 6.8), 4.6 mL glycerol (50%), 1.6 mL SDS (10%), 0.4 mL bromophenol blue (0.5%), 0.4 mL β-mercaptoethanol)) and boiling for 10 minutes. 15 µl samples were loaded on a 15% SDS-PAGE gel and proteins were separated by electrophoresis, transferred onto a PVDF transfer membranes (#88520, Thermo Scientific™) using Trans-Blot® Turbo™ Transfer System (Bio-Rad) and detected by anti-GST immunoblotting (GST Antibody (B-14) HRP, sc-138 HRP, Santa Cruz Biotechnology) or anti-His immunoblotting (His-probe Antibody (H-3) HRP, sc-8036 HRP, Santa Cruz Biotechnology).

Bimolecular Fluorescence Complementation (BiFC) assay

For BiFC assays, 20 ml cultures of *Agrobacterium tumefaciens* strain AGL1 harbouring constructs *pDEST–PID-VYCE, pDEST–CaM1-VYNE, pDEST–CML9-VYNE, pDEST–CML10-VYNE, pDEST–CML12-VYNE, pDEST–CML24-VYNE* or *pDEST-VYCE* were incubated in a 28°C shaker until an OD_{600} of 1.0 was reached. Bacteria were collected by centrifugation for 15 minutes at 4000 rpm, resuspended in 20 ml infiltration medium (10 mM $MgCl_2$, 10 mM MES/KOH, pH 5.7) supplemented with 200 µM Acetosyringone (Sigma-Aldrich, #D134406-5G), and incubated for at least 2 hours at 50 rpm at 28 °C on a table shaker in darkness. Agrobacterium strains each carrying one construct were mixed at equal volumes (5 ml each). Leaves of three weeks old *Nicotiana benthamiana* plants were infiltrated using a 5 ml syringe without needle. Two infiltrations per leaf, and a total of eight leaves from two plants were infiltrated. Two days later, infiltrated leaf parts were checked for YFP signal using the Zeiss LSM 5 Exciter 2C/1F Imager M1 (Zeiss, Oberkochen, Germany) confocal microscope, using a 20x objective. The YFP signal was detected using an argon 514 nm laser and a 530-600 nm band pass filter.

Accession numbers

Arabidopsis Genome Initiative locus identifiers for the genes mentioned are as follows: *CaM1/TCH1 (At5g37780), CaM2 (At2g41110), CaM3 (At3g56800), CaM4 (At1g66410), CaM5 (At2g27030), CaM6 (At5g21274), CaM7 (At3g43810), CML8 (At4g14640), CML9 (At3g51920), CML10 (At2g41090), CML11 (At3g22930), CML12/TCH3 (At2g41100), CML13 (At1g12310), CML14 (At1g62820), CML24/TCH2 (At5g377770), PID (At2g34650)*

Supplementary data:

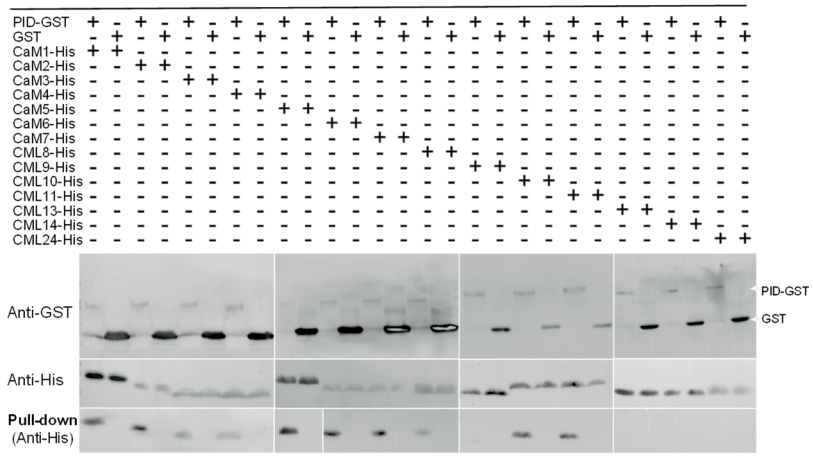

Figure S1. PID interacts with seven CaMs and the four most closely-related CMLs. *In vitro* pull-down using GST or GST-tagged PID bound to glutathione beads as bait, and HIS-tagged CaM or CML as prey. Upper panel: Western blot detecting input PID-GST or GST using anti-GST antibody. Middle panel: Western blot detecting input CaM-His or CML-His using anti-His antibody. Lower panel: Western blot detecting CaM-His or CMLs-His after pull-down using anti-His antibody.

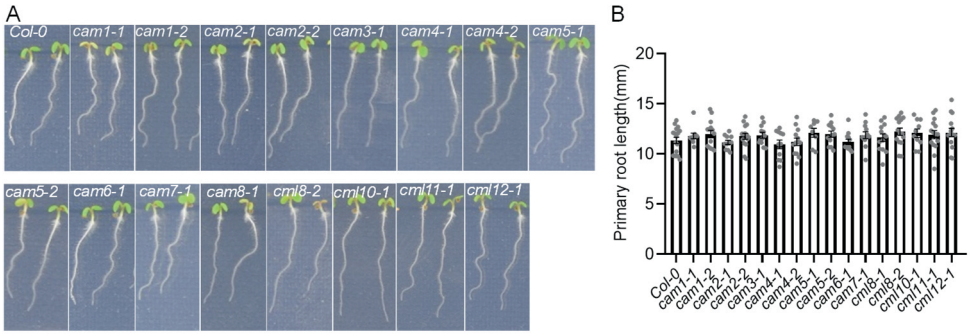

Figure S2. Seedling phenotype of different *cam or cml* loss-of-function mutant lines. (**A**). 5-day-old seedlings of *cam* or *cml* loss-of-function mutants grown on vertical plates containing agar medium. **(B)**. Quantitative analysis of the primary root length of the seedlings in (**A**).

Table S1 List of primers used for molecular cloning or mutant genotyping.

pCaM1 attB F	GGGGACAAGTTTGTACAAAAAAGCAGGCTCGAAGATTCTAAGAAATGGAT
pCaM1 attB R	GGGGACCACTTTGTACAAGAAAGCTGGGTGAGCTTCTTCGAGAAATCGTC

pCaM2 attB F	GGGGACAAGTTTGTACAAAAAAGCAGGCTCGGAATTCAGGGAAGCCTTCC
pCaM2 attB R	GGGGACCACTTTGTACAAGAAAGCTGGGTCTGTTTTTTCTTTTCTTTTCT
pCaM3 attB F	GGGGACAAGTTTGTACAAAAAAGCAGGCTCGCCATTCATGACGTCATTTC
pCaM3 attB R	GGGGACCACTTTGTACAAGAAAGCTGGGTCTGTTTTTTTCTTCTCCTTTT
pCaM4 attB F	GGGGACAAGTTTGTACAAAAAAGCAGGCTCGAAATAGACATGGCCAGTTT
pCaM4 attB R	GGGGACCACTTTGTACAAGAAAGCTGGGTCAGCTTCTTCTTCTCGTTTCT
pCaM5 attB F	GGGGACAAGTTTGTACAAAAAAGCAGGCTCGGACTAGACACAATAGTAGT
pCaM5 attB R	GGGGACCACTTTGTACAAGAAAGCTGGGTCTTTTTGGTTTAGATGAGAAA
pCaM6 attB F	GGGGACAAGTTTGTACAAAAAAGCAGGCTCGCACTCCGAATGTTCACCTC
pCaM6 attB R	GGGGACCACTTTGTACAAGAAAGCTGGGTCTTTCCTTCTTACCTTTTTTT
pCaM7 attB F	GGGGACAAGTTTGTACAAAAAAGCAGGCTCGAGACAGGTACCCACTTAAG
pCaM7 attB R	GGGGACCACTTTGTACAAGAAAGCTGGGTCTTTTTTTGTCTTCTTCGGAT
pCML8 attB F	GGGGACAAGTTTGTACAAAAAAGCAGGCTCGTGGTTCGTTAATTTGCTACG
pCCML8 attB R	GGGGACCACTTTGTACAAGAAAGCTGGGTCTGTTTTCTGAGAATATTTT
pCML9 attB F	GGGGACAAGTTTGTACAAAAAAGCAGGCTCGGCGCATTTTCATTAATTCG
pCML9 attB R	GGGGACCACTTTGTACAAGAAAGCTGGGTCATCTTCGATCACAAAGAAAA
pCML10 attB F	GGGGACAAGTTTGTACAAAAAAGCAGGCTCGAATGCACTTGCGAATCCCT
pCML10 attB R	GGGGACCACTTTGTACAAGAAAGCTGGGTCTGTTTTTTATTTTCTGTGAT
pCML11 attB F	GGGGACAAGTTTGTACAAAAAAGCAGGCTCGATGCATCATTTCCTCCCT
pCML11 attB R	GGGGACCACTTTGTACAAGAAAGCTGGGTCCCAATTAAAACTTGCTTAGT
pCML12 attB F	GGGGACAAGTTTGTACAAAAAAGCAGGCTCGAATGGTACATCAGTAACTT
pCML12 attB R	GGGGACCACTTTGTACAAGAAAGCTGGGTCTGTTTTTTTTGTTTTCTGTG
CaM2 attB R	5'GGGGACCACTTTGTACAAGAAAGCTGGGTTCACCTTAGCCATCATAACCTTCA3'
CaM2-stop attB R	5'GGGGACCACTTTGTACAAGAAAGCTGGGTCCTTAGCCATCATAACCTTCA3'
CaM3 attB F	GGGGACAAGTTTGTACAAAAAAGCAGGCTCGATGGCGGATCAGCTCACCG
CaM3 attB R	GGGGACCACTTTGTACAAGAAAGCTGGGTCTCACTTAGCCATCATGACCT
CaM3-stop attB R	GGGGACCACTTTGTACAAGAAAGCTGGGTCCTTAGCCATCATGACCTTAA
CaM4 attB F	GGGGACAAGTTTGTACAAAAAAGCAGGCTCGATGGCGGATCAGCTAACTG
CaM4 attB R	GGGGACCACTTTGTACAAGAAAGCTGGGTCTCACTTAGCCATCATAATCT
CaM4-stop attB R	GGGGACCACTTTGTACAAGAAAGCTGGGTCCTTAGCCATCATAATCTTGA
CaM5 attB F	GGGGACAAGTTTGTACAAAAAAGCAGGCTCGATGGCAGATCAGCTCACCG

CaM5 attB R	GGGGACCACTTTGTACAAGAAAGCTGGGTCTCAGAGAATACGGCAGTGAC
CaM5-stop attB R	GGGGACCACTTTGTACAAGAAAGCTGGGTCGAGAATACGGCAGTGACTTT
CaM6 attB F	GGGGACAAGTTTGTACAAAAAAGCAGGCTCGATGGCGGATCAGCTCACCG
CaM6 attB R	GGGGACCACTTTGTACAAGAAAGCTGGGTCTCACTTAGCCATCATGACTT
CaM6-stop attB R	GGGGACCACTTTGTACAAGAAAGCTGGGTCCTTAGCCATCATGACTTTGA
CaM7 attB F	GGGGACAAGTTTGTACAAAAAAGCAGGCTCGATGGCGGATCAGCTAACCG
CaM7 attB R	GGGGACCACTTTGTACAAGAAAGCTGGGTCTCACTTTGCCATCATGACTT
CaM7-stop attB R	GGGGACCACTTTGTACAAGAAAGCTGGGTCCTTTGCCATCATGACTTTGA
CML8 attB F	GGGGACAAGTTTGTACAAAAAAGCAGGCTCGATGGAAGAAACAGCACTGA
CML8 attB R	GGGGACCACTTTGTACAAGAAAGCTGGGTC TCAGTCAATGTTGATCATCA
CML8-stop attB R	GGGGACCACTTTGTACAAGAAAGCTGGGTC GTCAATGTTGATCATCATCT
CML9 attB F	GGGACAAGTTTGTACAAAAAAGCAGGCTTCATGGCGGATGCTTTCACAGATGAAG
CML9 attB R	GGGGACCACTTTGTACAAGAAAGCTGGGTCCTAATAAGAGGCAGCAATCATCA
CML9-stop attB R	GGGGACCACTTTGTACAAGAAAGCTGGGTCATAAGAGGCAGCAATCATCA
CML10 attB F	GGGGACAAGTTTGTACAAAAAAGCAGGCTTCATGGCGAATAAGTTCACTAG
CML10 attB R	GGGGACCACTTTGTACAAGAAAGCTGGGTCTCAAGAAAACAACGCTTCGAACA
CML10-stop attB R	GGGGACCACTTTGTACAAGAAAGCTGGGTCAGAAAACAACGCTTCGAACA
CML11 attB F	GGGGACAAGTTTGTACAAAAAAGCAGGCTTC ATGGCGGATCAGCTCACCG
CML11 attB R	GGGGACCACTTTGTACAAGAAAGCTGGGTCTTAACCATTGATCATCATCAT
CML11-stop attB R	GGGGACCACTTTGTACAAGAAAGCTGGGTCACCATTGATCATCATCAT
CML13 attB F	GGGGACAAGTTTGTACAAAAAAGCAGGCTCG ATGGGGAAAGATGGTCTGA
CML13 attB R	GGGGACCACTTTGTACAAGAAAGCTGGGTC TCACTTAGCAACCATCCTTG
CML13-stop attB R	GGGGACCACTTTGTACAAGAAAGCTGGGTC CTTAGCAACCATCCTTGCTA
CML14 attB F	GGGGACAAGTTTGTACAAAAAAGCAGGCTCG ATGAGCAAGGATGGTTTGA
CML14 attB R	GGGGACCACTTTGTACAAGAAAGCTGGGTC TTACTTAGCAACCATTCTAG
CML14-stop attB R	GGGGACCACTTTGTACAAGAAAGCTGGGTC CTTAGCAACCATTCTAGCAA
CML24 attB F	GGGGACAAGTTTGTACAAAAAAGCAGGCTTCATGTCATCGAAGAACGGAGTTG
CML24 attB R	GGGGACCACTTTGTACAAGAAAGCTGGGTCTCAAGCACCACCACCATTACTCA
CML24-stop attB R	GGGGACCACTTTGTACAAGAAAGCTGGGTCAGCACCACCACCATTACTCA
LBb1.3 for SALK lines	ATTTTGCCGATTTCGGAAC

Acknowledgements

The authors would like to thank Gerda Lamers and Joost Willemse for their help with the microscopy, Ward de Winter and Jan Vink for help with medium, tissue culture and plant caretaking. This author was supported by the China Scholarship Council.

Author contribution

Remko Offringa, Xiaoyu Wei designed the experiments, Xiaoyu Wei, Parjanya Kocherla, Linge Li, Yuanwei Fan performed the experiments and data analysis, Xiaoyu Wei and Remko Offringa wrote and finalization of the Chapter.

References

Antosiewicz, D. M., Polisensky, D. H., & Braam, J. (1995). Cellular localization of the Ca^{2+} binding TCH3 protein of Arabidopsis. Plant J. 8: 623-636.

Bailey, T. L., & Elkan, C. (1994). Fitting a mixture model by expectation maximization to discover motifs in biopolymers. Proc. Int. Conf. Intell. Syst. Mol. Biol. 2: 28-36.

Band, L. R., Wells, D. M., Larrieu, A., Sun, J., Middleton, A. M., French, A. P., ... & Bennett, M. J. (2012). Root gravitropism is regulated by a transient lateral auxin gradient controlled by a tipping-point mechanism. Proc. Natl. Acad. Sci. U.S.A. 109: 4668-4673.

Bassukas, A. E. L., Xiao, Y., & Schwechheimer, C. (2022). Phosphorylation control of PIN auxin transporters. Curr. Opin. Plant Biol. 65: 102146.

Batistic, O., Waadt, R., Steinhorst, L., Held, K., and Kudla, J. (2010). CBL-mediated targeting of CIPKs facilitates the decoding of calcium signals emanating from distinct cellular stores. Plant J. 61: 211–222.

Baum, G., Long, J. C., Jenkins, G. I., & Trewavas, A. J. (1999). Stimulation of the blue light phototropic receptor NPH1 causes a transient increase in cytosolic Ca^{2+}. Proc. Natl. Acad. Sci. U.S.A. 96: 13554-13559.

Benjamins, R., Ampudia, C.S., Hooykaas, P.J., & Offringa, R. (2003). PINOID-mediated signaling involves calcium-binding proteins. Plant Physiol. 132: 1623-1630.

Benjamins, R., Quint, A., Weijers, D., Hooykaas, P., & Offringa, R. (2001). The PINOID protein kinase regulates organ development in Arabidopsis by enhancing polar auxin transport. Development 128: 4057-4067.

Bennett, S. R., Alvarez, J., Bossinger, G., & Smyth, D. R. (1995). Morphogenesis in *pinoid* mutants of Arabidopsis thaliana. Plant J. 8: 505-520.

Boudsocq, M., & Sheen, J. (2013). CDPKs in immune and stress signaling. Trends Plant Sci. 18: 30-40.

Braam, J., & Davis, R. W. (1990). Rain-, wind-, and touch-induced expression of calmodulin and calmodulin-related genes in Arabidopsis. Cell 60: 357-364.

Cheng, H. Q., Han, L. B., Yang, C. L., Wu, X. M., Zhong, N. Q., Wu, J. H., Wang, F. X., Wang, H. Y., & Xia, G. X. (2016). The cotton MYB108 forms a positive feedback regulation loop with CML11 and participates in the defense response against Verticillium dahliae infection. J. Exp. Bot. 67: 1935–1950.

Cho, K. M., Nguyen, H. T. K., Kim, S. Y., Shin, J. S., Cho, D. H., Hong, S. B., ... & Ok, S. H. (2016). CML 10, a variant of calmodulin, modulates ascorbic acid synthesis. New Phytol. 209: 664-678.

Clough, S. J., & Bent, A. F. (1998). Floral dip: a simplified method for Agrobacterium-mediated transformation of Arabidopsis thaliana. Plant J. 16: 735-743.

Day, I. S., Reddy, V. S., Shad Ali, G., & Reddy, A. S. N. (2002). Analysis of EF-hand-containing proteins in Arabidopsis. Genome Biol. 3: 1-24.

Dela Fuente, R.K., and Leopold, A.C. (1973). A role for calcium in auxin transport. Plant Physiol. 51: 845-847.

den Dulk-Ras, A., & Hooykaas, P. J. (1995). Electroporation of Agrobacterium tumefaciens. Plant cell electroporation and electrofusion protocols, 63-72.

Dhonukshe, P., Huang, F., Galvan-Ampudia, C. S., Mähönen, A. P., Kleine-Vehn, J., Xu, J., ... & Offringa, R. (2010). Plasma membrane-bound AGC3 kinases phosphorylate PIN auxin carriers at TPRXS (N/S) motifs to direct apical PIN recycling. Development 137: 3245-3255.

Dindas, J., Scherzer, S., Roelfsema, M. R. G., von Meyer, K., Müller, H. M., Al-Rasheid, K. A. S., ... & Hedrich, R. (2018). AUX1-mediated root hair auxin influx governs SCFTIR1/AFB-type Ca^{2+} signaling. Nat. Commun. 9: 1-10.

Dong, Q., Wallrad, L., Almutairi, B. O., & Kudla, J. (2022). Ca^{2+} signaling in plant responses to abiotic stresses. J. Integr. Plant Biol. 64: 287-300.

Eklund, L., & Eliasson, L. (1990). Effects of calcium ion concentration on cell wall synthesis. J. Exp. Bot. 41: 863-867.

Fan, Y. (2014). The role of AGC3 kinases and calmodulins in plant growth responses to abiotic signals (Doctoral dissertation, Leiden University).

Felle, H. (1988). Auxin causes oscillations of cytosolic free calcium and pH inZea mays coleoptiles. Planta 174: 495-499.

Friml, J., Yang, X., Michniewicz, M., Weijers, D., Quint, A., Tietz, O., ... & Offringa, R. (2004). A PINOID-dependent binary switch in apical-basal PIN polar targeting directs auxin efflux. Science 306: 862-865.

Galván-Ampudia, C. S. (2009). Plant Agc protein kinases orient auxin-mediated differential growth and organogenesis (Doctoral dissertation, Leiden University).

Galván-Ampudia, C. S., & Offringa, R. (2007). Plant evolution: AGC kinases tell the auxin tale. Trends Plant Sci. 12: 541-547.

Galweiler, L., Guan, C., Muller, A., Wisman, E., Mendgen, K., Yephremov, A., & Palme, K. (1998). Regulation of polar auxin transport by AtPIN1 in Arabidopsis vascular tissue. Science 282: 2226-2230.

Gehl, C., Waadt, R., Kudla, J., Mendel, R. R., & Hänsch, R. (2009). New GATEWAY vectors for high throughput analyses of protein-protein interactions by bimolecular fluorescence complementation. Mol. Plant 2: 1051–1058.

Gehring, C. A., Irving, H. R., & Parish, R. W. (1990). Effects of auxin and abscisic acid on cytosolic calcium and pH in plant cells. Proc. Natl. Acad. Sci. U.S.A. 87: 9645-9649.

Geisler, M. M. (2021). A retro-perspective on auxin transport. Front. Plant Sci. 12: 756968.

Goh, C. S., Lee, Y., & Kim, S. H. (2012). Calcium could be involved in auxin-regulated maintenance of the quiescent center in the Arabidopsis root. J. Plant Biol. 55: 143-150.

Gomes, G. L. B., & Scortecci, K. C. (2021). Auxin and its role in plant development: structure, signalling, regulation and response mechanisms. Plant Biol. 23: 894-904.

Harmon, A. C., Gribskov, M., & Harper, J. F. (2000). CDPKs–a kinase for every Ca^{2+} signal? Trends Plant Sci. 5: 154-159.

Hasenstein, K. H., & Evans, M. L. (1986). Calcium dependence of rapid auxin action in maize roots. Plant Physiol. 81: 439-443.

Hepler, P.K. and Wayne, R.O. (1985) Calcium and Plant Development. Annual Review of Plant Physiol. 36: 397-439.

Huang, F., Kemel Zago, M., Abas, L., van Marion, A., Galván-Ampudia, C. S., & Offringa, R. (2010). Phosphorylation of conserved PIN motifs directs Arabidopsis PIN1 polarity and auxin transport. Plant Cell 22: 1129-1142.

Jing, X., Cai, C., Fan, S., Wang, L., & Zeng, X. (2019). Spatial and temporal calcium signaling and its physiological effects in Moso Bamboo under drought stress. Forests 10: 224.

Klee, C.B., Ren, H., and Wang, X. (1998). Regulation of calmodulin stimulated protein phosphatase, calcineurin. J. Biol. Chem. 273: 13367-13370.

La Verde, V., Dominici, P., & Astegno, A. (2018). Towards understanding plant calcium signaling through calmodulin-like proteins: A biochemical and structural perspective. Int. J. Mol. Sci. 19: 1331.

Lee, J. S., Mulkey, T. J., & Evans, M. L. (1984). Inhibition of polar calcium movement and gravitropism in roots treated with auxin-transport inhibitors. Planta 160: 536-543.

Lee, K., Thorneycroft, D., Achuthan, P., Hermjakob, H., and Ideker, T. (2010). Mapping plant interactomes using literature curated and predicted protein-protein interaction data sets. Plant Cell 22: 997–1005.

Lévy, J., Bres, C., Geurts, R., Chalhoub, B., Kulikova, O., Duc, G., ... & Debellé, F. (2004). A putative Ca^{2+} and calmodulin-dependent protein kinase required for bacterial and fungal symbioses. Science 303: 1361-1364.

Li, P., Zhao, C., Zhang, Y., Wang, X., Wang, X., Wang, J., ... & Bi, Y. (2016). Calcium alleviates cadmium-induced inhibition on root growth by maintaining auxin homeostasis in Arabidopsis seedlings. Protoplasma 253: 185-200.

Li, T., Yan, A., Bhatia, N., Altinok, A., Afik, E., Durand-Smet, P., ... & Meyerowitz, E. M. (2019). Calcium signals are necessary to establish auxin transporter polarity in a plant stem cell niche. Nat. Commun. 10: 1-9.

McCormack, E., Tsai, Y. C., & Braam, J. (2005). Handling calcium signaling: arabidopsis CaMs and CMLs. Trends Plant Sci. 10: 383-389.

Michniewicz, M., Zago, M. K., Abas, L., Weijers, D., Schweighofer, A., Meskiene, I., ... & Friml, J. (2007). Antagonistic regulation of PIN phosphorylation by PP2A and PINOID directs auxin flux. Cell 130: 1044-1056.

Monshausen, G. B., Miller, N. D., Murphy, A. S., & Gilroy, S. (2011). Dynamics of auxin-dependent Ca^{2+} and pH signaling in root growth revealed by integrating high-resolution imaging with automated computer vision-based analysis. Plant J. 65: 309-318.

Mroue, S., Simeunovic, A., & Robert, H. S. (2018). Auxin production as an integrator of environmental cues for developmental growth regulation. J. Exp. Bot. 69: 201-212.

Oh, M. H., Kim, H. S., Wu, X., Clouse, S. D., Zielinski, R. E., & Huber, S. C. (2012). Calcium/calmodulin inhibition of the Arabidopsis BRASSINOSTEROID-INSENSITIVE 1 receptor kinase provides a possible link between calcium and brassinosteroid signalling. Biochemical J. 443: 515-523.

Okada, K., Ueda, J., Komaki, M. K., Bell, C. J., & Shimura, Y. (1991). Requirement of the auxin polar transport system in early stages of Arabidopsis floral bud formation. Plant Cell 3: 677-684.

Olafsson, P., Wang, T., & Lu, B. (1995). Molecular cloning and functional characterization of the Xenopus Ca ($^{2+}$)-binding protein frequenin. Proc. Natl. Acad. Sci. U.S.A. 92: 8001-8005.

Patil, S., Takezawa, D., and Poovaiah, B. W. (1995). Chimeric plant calcium/calmodulin-dependent protein kinase gene with a neural visin-like calcium-binding domain. Proc. Natl. Acad. Sci. U.S.A. 92: 4897–4901.

Perochon, A., Aldon, D., Galaud, J. P., & Ranty, B. (2011). Calmodulin and calmodulin-like proteins in plant calcium signaling. Biochimie 93: 2048-2053.

Perochon, A., Dieterle, S., Pouzet, C., Aldon, D., Galaud, J. P., & Ranty, B. (2010). Interaction of a plant pseudo-response regulator with a calmodulin-like protein. Biochem. Biophys. Res. Commun. 398: 747-751.

Petrásek, J., Mravec, J., Bouchard, R., Blakeslee, J. J., Abas, M., Seifertová, D., ... & Friml, J. (2006). PIN proteins perform a rate-limiting function in cellular auxin efflux. Science 312: 914-918.

Plieth, C., & Trewavas, A. J. (2002). Reorientation of seedlings in the earth's gravitational field induces cytosolic calcium transients. Plant Physiol. 129: 786-796.

Popescu, S.C., Popescu, G.V., Bachan, S., Zhang, Z., Seay, M., Gerstein, M., Snyder, M., and Dinesh-Kumar, S.P. (2007). Differential binding of calmodulin-related proteins to their targets revealed through high-density Arabidopsis protein microarrays. Proc. Natl. Acad. Sci. U.S.A. 104: 4730-4735.

Raza, A., Ashraf, F., Zou, X., Zhang, X., & Tosif, H. (2020). Plant adaptation and tolerance to environmental stresses: mechanisms and perspectives. Plant Ecophysiology and Adaptation under Climate Change: Mechanisms and Perspectives I: General Consequences and Plant Responses, 117-145.

Robert, H. (2008). Calcium- and BTB domain protein-modulated PINOID kinase directs polar auxin transport. (Doctoral dissertation, Leiden University).

Rudd, J. J., & Franklin-Tong, V. E. (1999). Calcium signaling in plants. Cell. Mol. Life Sci. 55: 214-232.

Sanders, D., Pelloux, J., Brownlee, C., and Harper, J.F. (2002). Calcium at the crossroads of signaling. Plant Cell 14 (suppl.): S401-S417.

Sathyanarayanan, P. V., Cremo, C. R., & Poovaiah, B. W. (2000). Plant chimeric Ca^{2+}/calmodulin-dependent protein kinase: role of the neural visinin-like domain in regulating autophosphorylation and calmodulin affinity. J Biol. Chem. 275: 30417-30422.

Schirawski, J., Planchais, S., & Haenni, A. L. (2000). An improved protocol for the preparation of protoplasts from an established Arabidopsis thaliana cell suspension culture and infection with RNA of turnip yellow mosaic tymovirus: a simple and reliable method. J. Virol. Methods 86: 85-94.

Schulz, P., Herde, M., & Romeis, T. (2013). Calcium-dependent protein kinases: hubs in plant stress signaling and development. Plant Physiol. 163: 523-530.

Shih, H. W., DePew, C. L., Miller, N. D., & Monshausen, G. B. (2015). The Cyclic Nucleotide-Gated Channel CNGC14 Regulates Root Gravitropism in Arabidopsis thaliana. Curr. Biol. 25: 3119–3125.

Shishova, M., & Lindberg, S. (2004). Auxin induces an increase of Ca^{2+} concentration in the cytosol of wheat leaf protoplasts. J. Plant Physiol. 161: 937-945.

Sistrunk, M.L., Antosiewicz, D.M., Purugganan, M.M., & Braam, J. (1994). Arabidopsis TCH3 encodes a novel Ca^{2+} binding protein and shows environmentally induced and tissue-specific regulation. Plant Cell 6: 1553-1565.

Sun, L., Qin, J., Wu, X., Zhang, J., & Zhang, J. (2022). TOUCH 3 and CALMODULIN 1/4/6 cooperate with calcium-dependent protein kinases to trigger calcium-dependent activation of CAM-BINDING PROTEIN 60-LIKE G and regulate fungal resistance in plants. Plant Cell 34: 4088-4104.

Takezawa, D., Ramachandiran, S., Paranjape, V., and Poovaiah, B. W. (1996). Dual regulation of a chimeric plant serine threonine kinase by calcium and calcium calmodulin. J. Biol. Chem. 271: 8126–8132.

Tanaka, H., Dhonukshe, P., Brewer, P.B., and Friml, J. (2006). Spatiotemporal asymmetric auxin distribution: a means to coordinate plant development. Cell Mol. Life Sci. 63: 2738-2754.

Toyota, M., Furuichi, T., Tatsumi, H., & Sokabe, M. (2007). Hypergravity stimulation induces changes in intracellular calcium concentration in Arabidopsis seedlings. Adv. Space Res. 7: 1190-1197.

Toyota, M., Furuichi, T., Tatsumi, H., & Sokabe, M. (2008). Critical consideration on the relationship between auxin transport and calcium transients in gravity perception of Arabidopsis seedlings. Plant Signal. Behav. 8: 521-524.

Toyota, M., Furuichi, T., Tatsumi, H., & Sokabe, M. (2008). Cytoplasmic calcium increases in response to changes in the gravity vector in hypocotyls and petioles of Arabidopsis seedlings. Plant Physiol. 2: 505-14.

Ung, K. L., Winkler, M., Schulz, L., Kolb, M., Janacek, D. P., Dedic, E., ... & Pedersen, B. P. (2022). Structures and mechanism of the plant PIN-FORMED auxin transporter. Nature 609: 605-610.

Verma, S., Negi, N. P., Narwal, P., Kumari, P., Kisku, A. V., Gahlot, P., ... & Kumar, D. (2022). Calcium signaling in coordinating plant development, circadian oscillations and environmental stress responses in plants. Environ. Exp. Bot. 201: 104935.

Wang, J. P., Munyampundu, J. P., Xu, Y. P., & Cai, X. Z. (2015). Phylogeny of Plant Calcium and Calmodulin-Dependent Protein Kinases (CCaMKs) and Functional Analyses of Tomato CCaMK in Disease Resistance. Front. Plant Sci. 6: 1075.

Weinl, S., and Kudla, J. (2009). The CBL-CIPK $Ca(^{2+})$-decoding signaling network: Function and perspectives. New Phytol. 184: 517–528.

Wright, A. J., Knight, H., & Knight, M. R. (2002). Mechanically stimulated TCH3 gene expression in Arabidopsis involves protein phosphorylation and EIN6 downstream of calcium. Plant Physiol. 4: 1402-1409.

Xiao, Y. (2019). Novel factors modulating AGC kinase signalingcontrolled polar auxin transport. (Doctoral dissertation, Leiden University).

Xu, H., Heath, M.C. (1998). Role of calcium in signal transduction during the hypersensitive response caused by basidiospore-derived infection of the cowpea rust fungus. Plant Cell 4: 585–597.

Xu, T., Niu, J., & Jiang, Z. (2022). Sensing mechanisms: Calcium signaling mediated abiotic stress in plants. Front. Plant Sci. 13: 925863.

Yang, C., Li, A., Zhao, Y., Zhang, Z., Zhu, Y., Tan, X., ... & Mao, L. (2011). Overexpression of a wheat CCaMK gene reduces ABA sensitivity of Arabidopsis thaliana during seed germination and seedling growth. Plant Mol. Biol. Rep. 3: 681-692.

Yu, S., Wu, J., Sun, Y., Zhu, H., Sun, Q., Zhao, P., ... & Guo, Z. (2022). A calmodulin-like protein (CML10) interacts with cytosolic enzymes GSTU8 and FBA6 to regulate cold tolerance. Plant Physiol. 190: 1321-1333.

Zhang, J., Vanneste, S., Brewer, P. B., Michniewicz, M., Grones, P., Kleine-Vehn, J., ... & Friml, J. (2011). Inositol trisphosphate-induced Ca^{2+} signaling modulates auxin transport and PIN polarity. Dev. Cell 20: 855-866.

Zhang, L., & Lu, Y. T. (2003). Calmodulin-binding protein kinases in plants. Trends Plant Sci. 8: 123-127.

Zhao, X., Wang, Y.L., Qiao, X.R., Wang, J., Wang, L.D., Xu, C.S., & Zhang, X. (2013). Phototropins function in high-intensity blue light-induced hypocotyl phototropism in Arabidopsis by altering cytosolic calcium. Plant Physiol. 162: 1539-1551.

Zhu, X., Dunand, C., Snedden, W., & Galaud, J. P. (2015). CaM and CML emergence in the green lineage. Trends Plant Sci. 20: 483-48.

Zhu, X., Robe, E., Jomat, L., Aldon, D., Mazars, C., & Galaud, J. P. (2017). CML8, an Arabidopsis Calmodulin-Like protein, plays a role in Pseudomonas syringae plant immunity. Plant Cell Physiol. 58: 307-319.

Zimmermann, P., Hirsch-Hoffmann, M., Hennig, L., & Gruissem, W. (2004). GENEVESTIGATOR. Arabidopsis microarray database and analysis toolbox. Plant Physiol. 136: 2621-2632.